Astron. Astrophys. 231, 221–234 (1990)

ASTRONOMY AND ASTROPHYSICS

Solar line asymmetries and the magnetic filling factor ⋆

P. N. Brandt[1] **and S. K. Solanki**[2,3]

[1] Kiepenheuer-Institut für Sonnenphysik, Schöneckstr. 6, D-7800 Freiburg, Federal Republic of Germany
[2] Department of Mathematical Sciences, University of St. Andrews, St. Andrews KY16 9SS, Scotland
[3] Institut für Astronomie, ETH-Zentrum, CH-8092 Zürich, Switzerland

Received September 27, 1989; accepted January 18, 1990

Abstract. High quality spectra obtained in regions of varying activity near solar disk centre are analysed. Changes in line parameters (half-width, depth, equivalent width, wavelength at line bottom, bisector shape) are presented as a function of the magnetic filling factor. The filling factor is determined from a statistical analysis of line width following Stenflo and Lindegren (1977). Their technique is developed further. Its application to Stokes V data shows that the field strength within magnetic elements is relatively homogeneous.

The line depth is seen to decrease with increasing filling factor for all the observed lines, while the line width increases, even after the Zeeman broadening has been compensated for. For strong or temperature insensitive lines the equivalent width remains practically unchanged, but decreases for weak lines. The line bisectors show a marked change, with the lower part of the bisector straightening out, in accordance with results in the literature. The upper part of the bisector (i.e. $I > 0.7I_c$), in contrast, is observed to become more horizontal and redshifted, suggesting either larger downflow velocities or an increased weighting of the downflowing component of the atmosphere.

Line bisectors averaged over sets of 19 FeI lines and over several spectra of very small filling factor ($\alpha < 0.02$) show a blue shift of approx. 0.35 km/s, when referred to the MgI line λ5172.7 Å. With α increasing to ≥ 0.08 this blueshift decreases to 0.12 km/s at half the line depth.

The observations are qualitatively explained by a decrease in the contrast between the up- and downflow components of the non-magnetic part of the atmosphere in active regions ("abnormal granulation") coupled to either a decrease in the average temperature of the non-magnetic part, or a significant increase in small-scale velocity (line broadening velocity).

Key words: photosphere of the Sun – magnetic fields of the Sun – faculae of the Sun – convection – magnetic fields of stars

1. Introduction

The influence of magnetic fields on solar and stellar convection is of basic interest and has been widely studied theoretically (cf. reviews by e.g. Nordlund, 1986; Hughes and Proctor, 1988) and observationally (e.g. Mattig and Nesis, 1976; Livingston, 1982; Kaisig and Schröter, 1983; Brandt and Schröter, 1984; Miller et al., 1984; Title et al., 1986, 1989; Immerschitt and Schröter, 1987, 1989; Cavallini et al., 1985, 1988; Keil et al., 1989). Most of the observational investigations have been based on the difference between the "C"-shape and wavelength shift of photospheric lines in quiet and active regions on the Sun. The "C"-shaped asymmetry of the line bisectors and the shifts of spectral lines have been known for over 30 years (e.g. Schröter, 1957) and are usually attributed to the brightness-velocity correlation of the solar granulation (e.g. Beckers and Nelson, 1978; Kaisig and Durrant, 1982; Dravins et al., 1986).

Despite the relatively large number of investigations of line bisectors and shifts in active regions, which — besides some controversy (particularly regarding the line shifts) — have produced much interesting information, there is still a dire need for an investigation of the variation of the C-shape, wavelength shift and other line parameters of a *broad sample* of lines as a *quantitative function* of the magnetic flux. Such an investigation is the subject of the present paper. It should not only provide us with more information on how convection is locally affected by magnetic fields, but may also allow us to obtain an idea of whether this influence should be observable globally, i.e. on the Sun seen as a star ("integrated sunlight"). Long-term changes in C-shapes (Livingston, 1982, 1983) and equivalent width (Livingston and Holweger, 1982) of photospheric lines were derived from time series of spectra of integrated sunlight. These results have recently not been confirmed (Livingston and Huang, 1986; Livingston, 1987). However, the C-shape can also be observed in stellar spectra (Gray, 1982; Dravins, 1987) and is one of the very few diagnostics which can be used to infer convective motions on stellar surfaces. Therefore, the present investigation also serves as a guide to the expected magnitude of the changes in stellar bisectors caused by magnetic fields, which can cover sizeable fractions of the surface of some late type stars (e.g. Robinson et al., 1980; Marcy, 1984; Saar and Linsky, 1985; Saar, 1987; Mathys and Solanki, 1989). Despite its limited spatial resolution it seemed advisable to make use of the potential of the Fourier transform spectrometer ("FTS"; Brault

Send offprint requests to: P. N. Brandt
⋆ Mitteilungen aus dem Kiepenheuer-Institut Nr. 309

1978, 1985), whose advantages include a symmetric apparatus profile, a well defined wavelength scale, a high S/N ratio, and a low amount of scattered light. Additionally, this device offers the possibility to observe many lines strictly simultaneously. In this way, uncertainties due to solar and terrestrial line blends can be avoided and the results can be put onto a more solid statistical basis. The merits of this method have been reviewed recently by Solanki (1987a).

In the following, the recording of a series of FTS spectra of plage and quiet Sun regions and the method of deriving a magnetic filling factor for each of them, is described. For a set of 32 lines (mostly FeI) the line depth, equivalent width, halfwidth, and especially the bisectors are determined and the systematic changes of these parameters with the magnetic filling factor are investigated. The results are discussed, partly with the help of simple model calculations, and with reference to the findings of other authors concerning the structure of the upper convection zone in the presence of magnetic fields.

2. Observations

All observations were performed with the McMath solar telescope at Kitt Peak National Observatory (Tucson) in the period June 1 to 13, 1984. With the aid of the daily magnetograms and an improvised slit-jaw viewing system, using an Hα-Daystar filter, plage and quiet regions were selected on the solar disk. On several days plage regions were scanned in a stepwise manner, using the limb guiding system, across the 5 by 25 arcsec^2 entrance slit of the FTS, so that consecutive spectra outside and at several positions in plages were obtained. Pores and sunspots were carefully avoided.

Two-sided interferograms, with a theoretical resolving power corresponding to $\lambda/\Delta\lambda \simeq 200\,000$, and integration times of 13.7 min, were obtained with the FTS. For some spectra twice as long integration times were used. After Fourier transformation spectra were obtained, which cover the usable spectral range $\lambda\lambda$5050 to 6650Å, or 19 800 to 15 000 cm^{-1}, at a step width of 0.026 cm^{-1}.

A set of 25 spectra observed close to disk centre in the range $1.0 \geq \cos\theta \geq 0.9$ was selected for further evaluation in the present work. According to the comparison with the magnetograms they cover a wide range of activity and include 6 spectra taken at disk centre in quiet regions on different days.

3. Estimate of the absolute amount of magnetic flux

3.1. The Stenflo-Lindegren method

The magnetic filling factor is estimated with the method originally developed by Stenflo and Lindegren (1977) to set an upper limit on the turbulent magnetic field and later used by Mathys and Solanki (1989) to measure stellar magnetic fields. This method is based on a multi-variate regression of a line parameter (of the unpolarized profile) sensitive to Zeeman splitting. Thus, for a large number of spectral lines of the same ion, the generally small effects due to the magnetic field can be isolated and thereby some information obtained on the filling factor. We shall follow Stenflo and Lindegren (1977) and use the line width at half minimum, v_D, given in velocity units (defined as the Doppler width of a Gaussian having the same width at half minimum). After the continua of the raw spectra have been normalized and the relevant line parameters determined, a regression of the following form is carried out:

$$v_D = x_0 + x_1 v_m^2 \lambda^2/v_0 + x_2\langle v_m^2\rangle\lambda^2/v_0 + x_3 S + \\ + x_4 S^2 + x_5 \chi_e v_0, \tag{1}$$

where $x_0, \ldots, x_5$ are regression coefficients, S is the line strength, χ_e is the excitation potential, λ the wavelength, v_0 is an approximation of v_D, $v_0 = y_0 + y_1 S^2$, and

$$v_m^2 = (g_{\text{eff}}^2 + x_\sigma)\frac{(1+\cos\gamma^2)}{2} + x_\pi \frac{\sin\gamma^2}{2}, \tag{2}$$

for a magnetic field at an angle γ to the line of sight. $\langle v_m^2\rangle$ is averaged over all the lines. In Eq. (2) g_{eff} is the effective Landé factor of the line, and

$$x_\pi = (g_1 - g_2)^2(3s - d^2 - 2)/10, \\ x_\sigma = (g_1 - g_2)^2(8s - d^2 - 12)/80, \tag{3}$$

with

$$s = J_1(J_1+1) + J_2(J_2+1), \\ d = J_1(J_1+1) - J_2(J_2+1) \tag{4}$$

(c.f. Landi Degl'Innocenti, 1982, 1985; Mathys and Stenflo, 1986). In Eqs.(3) and (4) J_1 and g_1 are the angular momentum quantum number and the Landé factor of the lower level of the line, respectively. J_2 and g_2 are the respective quantities for the upper level. These extra elements in the magnetic (x_1) term of the regression take the anomalous Zeeman splitting into account and have been listed by Landi Degl'Innocenti (1985) for the 400 unblended FeI lines selected by Stenflo and Lindegren (1977). For more details on the derivation of Eq. (1), and tests on the validity of the results derived with it, see Stenflo and Lindegren (1977) and Mathys and Solanki (1989).

If we take the intermittency of the magnetic field into account by assuming a simple two component model composed of a magnetic component of field strength B covering a fraction α of the surface in the resolution element and a non-magnetic component covering the remainder, $1-\alpha$, then the filling factor α is coupled to the regression coefficient x_1 of the Zeeman splitting term via

$$\alpha = \frac{x_1}{k^2 c^2 B^2 \delta_c \delta_l} \tag{5}$$

where $k = 4.67\,\text{km}^{-1}\text{G}^{-1}$, c is the speed of light, $\delta_c = I_c^{\text{magnetic}}/I_c^{\text{quiet Sun}}$ is the continuum contrast of the magnetic elements relative to the quiet Sun, and δ_l is the average amount of line weakening in the magnetic elements due to their generally higher temperature.

If δ_l, δ_c, and B are known, then the filling factor α can be determined directly from Eq.(5). Tarbell and Title (1977) and Stenflo and Harvey (1985) have shown that the magnetic field strength in fluxtubes is practically independent of the filling factor. We can therefore use the same value of B for all spectra. Probably the magnetic field strength most relevant to the present analysis is the one determined by Solanki and Stenflo (1984). They applied a similar statistical approach on Stokes V data, so that their B values should refer to roughly the level in the atmosphere we require, i.e. to the level at which the weakest FeI lines are formed. For 5 regions they find B values ranging

between 1400 and 1700 G. Similar, if not greater, uncertainties also exist as far as δ_l and δ_c are concerned. For example, the values of δ_l depend on the filling factor (cf. Solanki and Stenflo, 1984 1985), and even on the wavelength interval used for the analysis (since lines of different excitation potential and strength are distributed unevenly over λ). Values of δ_c are also highly uncertain, with values ranging from 1.0 (e.g. Chapman, 1970) to 2.0 (Koutchmy, 1977) being found in the literature. Furthermore, δ_c may also be a function of α. We have used the 182 unblended FeI lines between 5400 Å and 6650 Å which have line strengths (as defined by the area of the lower half of the line) less than 8 F. Assuming $B = 1500$ G, $\delta_c = 1.4$, and $\delta_l = 0.7$ we have obtained values of α ranging from 0.00 to 0.12 (sometimes also quoted as 0 to 12%) for the 25 spectra that were analyzed. The choice of δ_c is compatible with the results of Muller and Keil (1983) and Schüssler and Solanki (1988). The accuracy of our absolute values of α is not better than $\pm 50\%$, due to the cumulative effect of the uncertainties in x_1, B, δ_c, and δ_l. However, the internal consistency of our results is considerably better than this, since it only depends on how strongly B, δ_c, and δ_l vary with filling factor, as well as on the uncertainty of x_1. We therefore feel that the α scales in the figures may have to be stretched or compressed by a considerable amount, but that the relative positions of the points should remain relatively independent of our choice (to within approximately 0.02 on the adopted α scale).

We wish to emphasize that the determination of the filling factor from a polarimeter (e.g. magnetograph) recording faces similar problems (Solanki, 1985; Grossmann-Doerth et al., 1987). The Stokes I regression analysis approach actually has the advantage that it measures the squared average magnetic field and not only the net line of sight magnetic flux. It, therefore, gives the correct value even in the extreme case when equal amounts of negative and positive polarity field exactly compensate each other, so that a polarimeter would give a filling factor of zero. The main disadvantage of the Stenflo-Lindegren method is that it has a smaller sensitivity than polarimetric techniques.

3.2. *Other indicators of the filling factor*

The Stenflo-Lindegren technique is in fact an indicator of $\sqrt{\alpha}\,B$ and we can derive α from it only by assuming some value for B. We now wish to briefly outline a method for determining the filling factor directly from the unpolarized line profiles. One should note that a relatively large magnetic field strength and a small filling factor affect a line profile quite differently from a weak field with a large α, even if $\sqrt{\alpha}\,B$ is the same for both. In the latter case practically the complete line profile is broadened as if two Gaussians had been slightly shifted against each other. In the case of a small filling factor, on the other hand, the part of the profile near the continuum is broadened much more than the part near the core. This means that if we measure the width at different levels in the lines, and carry out a regression at each level, then the ratio of the Zeeman regression coefficients should be a measure of the filling factor. If $v_D(nd)$ is the line width at a level nd above line bottom, with d being the line depth and $0 < n < 1$, and $x_1(nd)$ is the regression coefficient of the Zeeman term of the regression equation to $v_D(nd)$, then $x_1(nd)/x_1(md)$, $(n \neq m)$ is a measure of the filling factor. We have determined x_1 at three different levels in the line, i.e. $0.3d$, $0.5d$, and $0.7d$ above line bottom, for all the regions studied in this paper and additionally for 4 FTS Stokes I and V spectra of active regions and the network obtained near disk centre (cf. Stenflo et al., 1984). In Fig. 1a we have plotted $x_1(0.7d)/x_1(0.5d)$ vs. $x_1(0.5d)$, while in Fig. 1b $x_1(0.3d)/x_1(0.5d)$ vs. $x_1(0.5d)$ is shown. The fact that the two curves are monotonic implies that $x_1(0.5d)$ alone is indeed a measure of the filling factor. The arrows at the right mark the values for two regions with $x_1(0.5d) = 6.7 \cdot 10^{17}$ and $9.9 \cdot 10^{17}$.

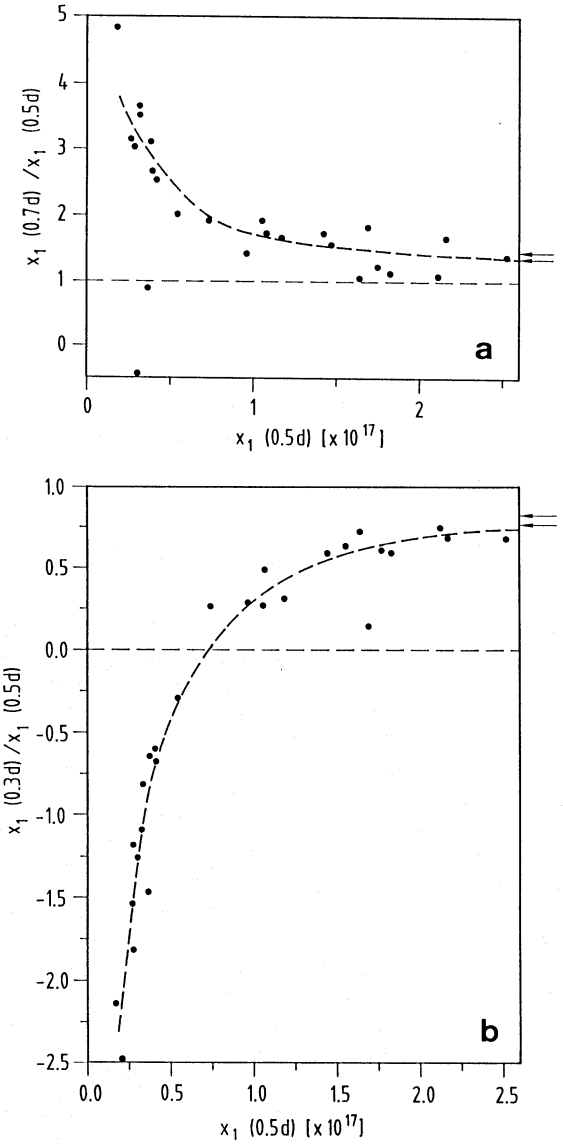

Fig. 1a,b. Ratios of regression coefficients for Zeeman splitting at different levels of the line profile.

We are also in the fortunate position of being able to test how these two indicators behave for α close to 1. To this end we have taken the integrated Stokes V profile, which is an approximation of the Stokes I profile inside magnetic features (Solanki and Stenflo, 1984; Solanki, 1987b). In a two component model this line profile should have a shape corresponding to $\alpha = 1$ (since it gets no contribution from the non-magnetic parts of the atmosphere). When we apply the method described above to this profile, we do indeed obtain $x_1(0.7d)/x_1(0.5d) \approx x_1(0.3d)/x_1(0.5d) \approx 1$. Besides verifying the intuitive expectations, this result also limits the amount of net flux in weak field (less than a few hundred G) and very strong field form (say 2500 G

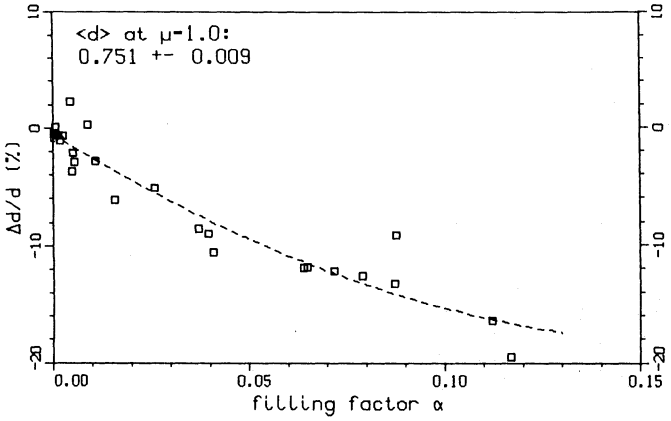

Fig. 2. Variation of line depth of FeI λ5250.2 Å as function of the magnetic filling factor α.

or more) to less than 10-20% of the net flux in these regions, in accordance with the results of Solanki et al. (1989) and Zayer et al. (1989).

It should be noted that so far this method is qualitative. It can, however, be transformed into a quantitative diagnostic by either calibrating it with radiative transfer line profile calculations or other observations. However, in the present paper it only serves to illustrate the reliability of x_5 as a filling factor diagnostic and we shall not go into further details here.

Another indicator for the amount of magnetic flux is the line depth of a temperature and/or magnetic field sensitive line. An ideal line is FeI λ5250.2 Å, since it is extremely temperature sensitive (χ_e = 0.12 eV) and in addition also has a large Zeeman splitting. Therefore, its depth changes quite rapidly with filling factor as can be seen in Fig. 2. A similar plot, but with the Stokes V amplitude of λ5250.2 Å as abscissa has also been published by Stenflo and Harvey (1985). Fig. 2 may be used to derive "filling factors" without having to measure many lines or Stokes V. However, before using this curve to determine the approximate filling factor, stray light and spectral resolution should be compensated for, since otherwise spuriously large values of α would be obtained.

4. Selection of lines and evaluation procedure

For the rest of the present investigation a set of 32 weak to medium-strong lines (mostly FeI) have been selected. They are listed in Table 1 and, for the sake of comparison, comprise 3 FeI lines around λ6300 Å studied by Cavallini et al. (1985), the set of 11 lines in the range λ6232–6265 Å used by Gray (1982) in a study of convective velocities in stars, the set of 10 FeI lines studied by Livingston (1983, 1984) and the 6 FeI lines studied by Kaisig and Schröter (1983). Additionally Mg λ5173 Å and 8 O_2 lines around λ6300 Å have been chosen as wavelength references.

In order to correct for trends in the continuum, in each spectrum subinterval of approximately 35 Å width all values were normalized to the point of highest intensity and a linear correction of $\approx$ 0.045% per 1 Å was applied; this correction was determined from a low resolution overall spectrum supplied with each of the spectra and accounted for real continuum variations and changes of predisperser transmission and photodiode response as function of wavelength. Additionally, the quasi-continuum in the far wing of each line was corrected to yield the value given in the atlas by Kurucz et al. (1984). Usually corrections of < 1% were necessary.

Table 1. List of lines used for the present analysis; g_{eff} values from Solanki and Stenflo (1985), and Livingston and Holweger (1982); excitation potential χ_e from Stenflo and Lindegren (1977). $\langle W \rangle$ = line equivalent width (in mÅ) averaged over 6 spectra recorded at disk centre with $\alpha < 0.02$; $\langle d \rangle$ = same average for line depth; σ_d = r.m.s. scatter of $\langle d \rangle$; $\Delta d/d$ = variation of line depth from $\alpha < 0.02$ to $\alpha = 0.12$ relative to the line depth in the quiet Sun; $\Delta W/W$ and $\Delta F/F$ corresponding values for equivalent width and full width at half line depth; $\Delta\lambda_{\nabla q}$ = line bisector asymmetry between line minimum and $I/I_c = 0.7$ for $\alpha < 0.02$ ('quiet'); $\Delta\lambda_{\nabla a}$, the same for $\alpha = 0.12$ ('active'), cf. Sect. 5.5.

* = lines used for the analysis of averaged bisector wavelength positions, cf. Sect. 5.6.

No. el.	λ [Å]	g_{eff}	χ [eV]	⟨W⟩ [mÅ]	⟨d⟩	σ_d	Δd/d [%]	ΔW/W [%]	ΔF/F [%]	$\Delta\lambda_{\nabla q}$ [mÅ]	$\Delta\lambda_{\nabla a}$ [mÅ]
1 FeI	6302.5*	2.50	3.69	93.1	0.667	0.005	-13.7	-3.7	13.3	3.6	3.2
2 FeI	6301.5*	1.67	3.65	142.7	0.734	0.003	-8.3	-1.6	10.3	5.6	2.1
3 FeI	6297.8*	1.00	2.22	78.3	0.665	0.005	-10.9	-4.7	5.9	2.9	2.0
4 FeI	6265.1*	1.58	2.18	91.4	0.707	0.004	-10.9	-3.4	8.7	3.9	2.6
5 FeI	6256.4	-	2.45	97.4	0.704	0.003	-9.5	-5.5	4.4	6.8	4.8
6 FeI	6252.6*	1.08	2.40	131.0	0.759	0.004	-6.5	-1.4	5.8	3.4	-0.3
7 VI	6251.8	-	0.29	15.5	0.124	0.003	-13.7	-9.9	2.5	-	-
8 FeII	6247.6	1.10	3.89	58.5	0.488	0.005	-3.9	0.7	4.6	2.0	1.2
9 FeI	6246.3*	1.58	3.60	139.9	0.734	0.003	-8.3	-2.0	9.5	5.6	2.4
10 ScII	6245.6	-	1.51	35.9	0.319	0.004	-9.2	-7.0	2.7	-	-
11 SiI	6244.5	-	5.61	54.0	0.343	0.003	-8.4	-6.1	2.3	0.0	0.2
12 FeI	6240.7	1.00	2.22	48.5	0.507	0.009	-13.6	-10.1	2.9	0.8	0.8
13 SiI	6237.3	-	5.61	77.7	0.409	0.004	-8.6	-5.7	3.1	-1.2	-0.8
14 FeI	6232.6*	2.00	3.65	94.3	0.662	0.004	-12.3	-3.2	11.0	3.2	2.6
15 FeI	5855.1	0.62	4.61	23.6	0.236	0.004	-6.8	-6.6	-1.4	-	-
16 FeI	5635.8	0.67	4.26	39.7	0.381	0.007	-8.6	-7.2	1.0	0.3	0.2
17 FeI	5576.1*	0.00	3.43	147.5	0.794	0.004	-5.8	-3.1	4.3	4.0	0.0
18 FeI	5560.2	0.62	4.42	56.2	0.548	0.007	-8.3	-5.6	2.1	1.3	0.9
19 FeI	5506.8*	2.00	0.99	129.9	0.837	0.006	-6.4	2.2	10.3	4.5	0.1
20 FeI	5434.5*	0.00	1.01	196.6	0.876	0.007	-4.9	-0.9	5.9	4.7	-2.9
21 FeI	5395.2	0.50	4.44	23.9	0.239	0.005	-6.6	-5.8	-2.1	-	-
22 TiII	5381.0	0.90	1.60	65.7	0.591	0.004	-5.9	-3.2	2.7	1.6	0.9
23 FeI	5379.6*	1.00	3.69	64.9	0.647	0.006	-9.2	-6.3	3.0	2.0	1.2
24 FeI	5302.3*	1.50	3.28	170.2	0.831	0.005	-5.9	-1.1	6.8	5.3	0.3
25 FeI	5263.3*	1.50	3.26	148.7	0.823	0.004	-6.1	-1.8	6.5	4.8	0.4
26 FeI	5250.7*	1.50	2.20	126.2	0.816	0.004	-6.7	-1.5	7.0	4.8	2.0
27 FeI	5250.2*	3.00	0.12	69.1	0.751	0.009	-16.7	-7.6	9.5	2.6	2.5
28 FeI	5217.4*	1.50	3.21	126.9	0.813	0.004	-6.6	-1.0	7.2	5.8	1.8
29 FeI	5198.7*	1.50	2.22	102.6	0.813	0.005	-6.9	-0.5	6.9	4.8	2.5
30 FeI	5137.4*	1.20	4.18	133.9	0.815	0.003	-6.1	-2.8	5.9	5.9	2.9
31 FeI	5123.7	0.00	1.01	116.4	0.845	0.005	-5.4	-2.3	4.1	-0.2	-3.4
32 FeI	5074.8*	0.90	4.22	140.9	0.834	0.004	-5.5	-2.0	5.2	5.8	1.9

For ease of treatment the intensity data in spectral intervals of $\pm$1.2 Å around the selected lines were interpolated by use of a Fourier interpolation technique ('zero filling') to yield values at 1/4 of the original wavenumber stepwidth, i.e. at 0.0065 cm^{-1} corresponding to $\Delta\lambda$ between 1.7 and 2.6 mÅ. This procedure left both the given spectral resolution and the S/N ratio of 2000 to 3000 of the original data points unchanged (Brault and White, 1971). Bisector points were then calculated by computing the second order polynomial for three intensity points in each flank of the line in steps of 2% of the continuum intensity, starting at the lowest even percent value above line minimum and ending at relative intensity 0.92. All graphic bisector presentations in the following also start and end at these levels. No other smoothing or interpolation was applied. Line depths were determined by fitting second order polynomials into the lowest eighth of the line profiles and computing their minima.

The spectral windows used for the determination of the equivalent width in most cases were limited by the appearance of blends in the line wings. Thus for the weaker lines typical windows of the order of $\pm$0.2 Å, for the stronger ones two or three times this value was used, so that the far wings of the lines were neglected.

The absolute wavelength scale of the FTS was checked by the following procedure. In each spectrum the average difference of the vacuum wavenumbers of 8 terrestrial O_2 lines in the

range λ6280 to 6306 Å (or 15918 to 15852 cm^{-1} in vacuum wavenumbers) to the values quoted by Babcock and Herzberg (1948) and by Pierce and Breckinridge (1973) was determined. Values in the range +0.003 and −0.021 cm^{-1} were found. To correct for these differences, all vacuum wavenumbers were then multiplied by a so-called "rubber scale factor" (cf. also Palmer and Engleman, 1983), typically ranging between 0.9999998 and 1.0000013 for the different spectra. Furthermore, the dispersion of the FTS, which is intrinsically determined by the stabilized reference laser, was checked and found to be correct within approx. $\pm 3 \cdot 10^{-7}$, by the comparison of a set of 22 solar lines covering the whole wavelength range with the values tabulated by Pierce and Breckinridge (1973).

5. Results

In the following, the results for regions of different magnetic filling factors will be presented. The discussion of the results, their comparison with those of other investigations and their interpretation will be deferred to Section 6. In order to judge the reliability of the results, we first discuss the stability of the data and their possible impairment by insufficient spatial and/or temporal averaging and by photometric noise. A preliminary version of a part of the results had been presented by Brandt and Solanki (1987).

5.1. Data stability and noise

Temporal and spatial variations of the physical parameters, like temperature or velocity, due to the granulation or oscillation patterns are well established facts in solar physics. The FTS entrance slit of 5 by 25 $arcsec^2$ performs a spatial averaging over approx. 50 granules and several oscillation elements. Additionally, the integration time of 13.7 min yields a temporal averaging over approx. one granular lifetime and approx. three cycles of the oscillation. Which criterion can be used to judge the stability of the results?

As one criterion one can obviously use the agreement between the 6 measurements taken on 4 different days at disk centre in regions with filling factors < 0.02. As can be seen from Table 1, the typical r.m.s. scatter of the *line depth* among these 6 spectra is of the order of 0.005 in units of the continuum. Similarly, but not shown on Table 1, the r.m.s. scatter values of both the *line halfwidth* and the *equivalent width* range between 0.5% and 1%. These variations, which contain contributions of solar as well as of instrumental origin, indicate that apparently the temporal and spatial averaging performed in each spectrum was sufficient to obtain a very stable sample.

Also the *shapes of the bisectors* turn out to be very stable in this set of disk centre observations. As an example, Fig. 3 shows the 6 bisectors for the FeI line λ5576.1 Å shifted relative to each other such as to coincide in the intermediate range of relative intensities 0.4 to 0.7. The r.m.s. scatter of the bisector positions in this intermediate range is $\approx$ 0.08 mÅ. It increases to $\approx$ 0.17 mÅ towards line minimum and to approx. 0.5 mÅ at relative intensity 0.9. One can easily estimate, what fraction of this scatter is due to the photometric noise in the measurements. Following the argument by Brandt and Nesis (1973), the uncertainty of the position of the line wing $\delta\lambda$ can be derived from the uncertainty of the intensity values $\delta I/I$ (given by the reciprocal S/N ratio of the measurement) via the intensity gradient of the line profile

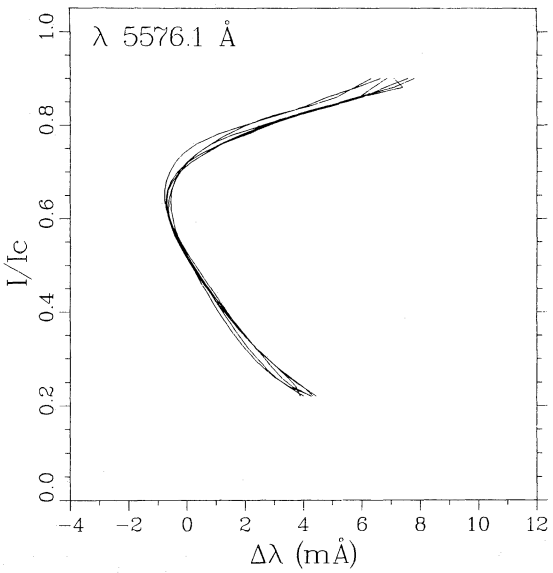

Fig. 3. Bisectors of the line FeI λ5576.1 Å observed at disk centre for filling factors $\alpha < 0.02$. The 6 bisectors were shifted relative to each other for best coincidence to show the variations of bisector shape only.

$1/I \cdot dI/d\lambda$. Assuming that n independent points are averaged in order to determine the corresponding section of the line profile, and keeping in mind that the bisector is calculated as a wavelength difference from opposite line wings (which increases the uncertainty by a factor of $\sqrt{2}$), one obtains

$$\delta\lambda = \frac{I\sqrt{2}}{(dI/d\lambda)\,(S/N)\,\sqrt{n}} \cdot \tag{6}$$

Inserting the gradient of the line profile λ5576.1 Å at relative intensity 0.9 of 0.0015 $mÅ^{-1}$, a S/N ratio of 2500, and assuming an averaging over three measurement points, one obtains $\delta\lambda \approx$ 0.2 mÅ as an estimate for the r.m.s. wavelength scatter of the bisector. This means, that about one half of the scatter of the bisectors in the uppermost part of Fig. 3 is due to the photometric noise of the measurements and that the other half represents real variations of solar origin.

5.2. Variation of the line depth

The average line depths for the 6 spectra taken at disk centre in regions with very small filling factor ($\alpha < 0.02$) are given in Table 1. It is noteworthy that all our values are approx. 1.7% larger than those in the Jungfraujoch-Atlas (Delbouille et al., 1973) as given by Dravins et al. (1981) — except for the value for λ5250.2 Å, which is 3.7% larger in our sample. The general difference very probably is due to a different continuum assignment in the two observations. The larger difference for λ5250.2 Å, however, may be explained by some slight activity which was overlooked, when the corresponding section of the Jungfraujoch-Atlas was recorded. In Fig. 2 it was demonstrated how sensitively this line's depth decreases with increasing filling factor. For $\alpha < 0.02$ a line depth of 0.751 ± 0.009 should be used for λ5250.2 Å.

The weakening of medium-strong lines in regions of increased magnetic field had been observed already more than 20 years ago in spectra and spectroheliograms of medium to high spatial

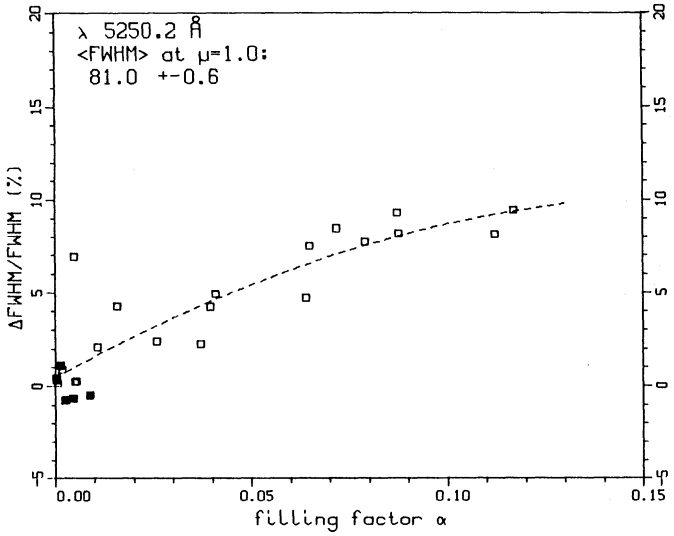

Fig. 4. Change of the line width (FWHM) of FeI λ5250.2 Å as function of the magnetic filling factor α.

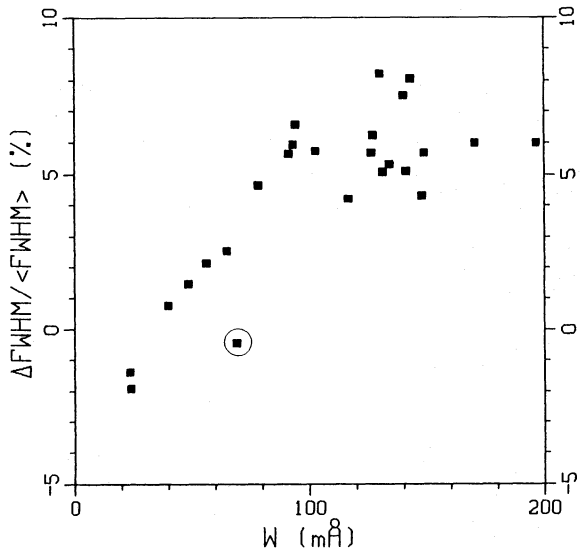

Fig. 5. Change of the line width (FWHM) between $\alpha < 0.02$ and $\alpha = 0.12$ as function of the equivalent width after subtraction of Zeeman broadening. The 'magnetograph line' FeI λ 5250.2 mÅ is encircled.

resolution (e.g. Beckers and Schröter, 1968; Chapman and Sheeley, 1968). While Beckers and Schröter (1968) interpret these so-called 'line gaps' as mainly due to the Zeeman splitting of lines with large Landé factors, Chapman and Sheeley (1968) notice that they also occur in lines with small or zero Landé factors, like λ5576.1 Å.

Our FTS spectra, which represent a spatial average of 5 by 25 arcsec^2, also show a consistent decrease of the line depth with increasing filling factor for lines with large as well as those with small or zero Landé factor. The large change of line depth of approx. −17% for the g=3 line FeI λ5250.2 Å had already been demonstrated in Fig. 2. For the stronger g=0 line λ5576.1 Å a change of only −6% is found when α varies from < 0.02 to 0.12. For the other lines the relative changes of the line depth $\Delta d/d$ (in %) for α varying from < 0.02 to 0.12, were determined from fit parabolae of the type shown in Figure 2. They are listed in Table 1 for all 32 lines investigated.

5.3. *Variation of the line halfwidth*

Additionally to the observed line weakening, most lines show a consistent increase of the full width at half line minimum (FWHM, abbreviated F) with increasing filling factor. As an example, Fig. 4 shows the relative change of the FWHM as a function of the filling factor for the 'magnetograph line' λ5250.2 Å. Between $\alpha < 0.02$ and 0.12 the FWHM increases by 9.5% for this line. The other FeI lines change by −1.6% to approx. +14%. Of course, here again part of the increase of the FWHM is due to the effect of Zeeman splitting. However, if one estimates the amount of line broadening from the second term of Eq. (1) in the form

$$\frac{\Delta F}{F_0} = \frac{F - F_0}{F_0} = x_1 g_{\text{eff}}^2 \lambda^2 / v_0^2 \qquad (7)$$

using the x_1 values derived from the data and taking the other line parameters from either Table 1 or the table by Stenflo and Lindegren (1977), one can subtract this magnetic broadening from the experimental values found in this investigation. In Fig. 5, the residual values of line broadening found in this way are plotted as a function of the equivalent width W. The graph shows a conspicuous trend of the line broadening with W, with values around or even below zero at small values of the equivalent width and an increase to values between 5 and 8.5% for the stronger lines. The 'magnetograph line' after correction for Zeeman broadening shows a change of approximately zero. Of course, for the three $g = 0$ lines of the set, no correction had to be applied. Their halfwidths increase by between 4 and 6% (cf. Table 1), which is consistent with the increases of other lines in our sample having similar W, after the effect of Zeeman broadening has been removed.

5.4. *Variation of the equivalent width*

For each line an average equivalent width $\langle W \rangle$ was computed from the 6 disk centre spectra taken in regions of very low activity ($\alpha < 0.02$). These average values are listed in Table 1. If one converts the values to $\langle W \rangle / \lambda$, the reduced equivalent width, and compares them with the values given in the Rowland Tables (Moore et al., 1966) it turns out that most of our values consistently are between 10 and 20% larger than the former. This discrepancy of the Rowland Tables to more modern data is well known (Griffin, 1969; Balthasar, 1984).

In order to determine the systematic variation of the equivalent width with the filling factor, graphs of the type shown in Fig. 6 were made and the relative change of the equivalent width derived from the values of second order polynomial fits at $\alpha = 0$ and 0.12. The majority of the lines show a marked and systematic decrease of the equivalent width. In Fig. 7 the result is summarized for all lines of the investigated set by plotting the relative change of the equivalent width as a function of the equivalent width in the quiet Sun. Obviously, the weakest lines show the strongest *decrease* of the equivalent width with increasing filling factor. No essential difference can be seen between lines of high excitation potential ($\chi_e > 2.0$ eV, squares) and those of low excitation potential ($\chi_e \leq 2.0$ eV, triangles). The only exceptions are the FeI line λ6247.6 Å and the FeI line λ5506.8 Å. The strong

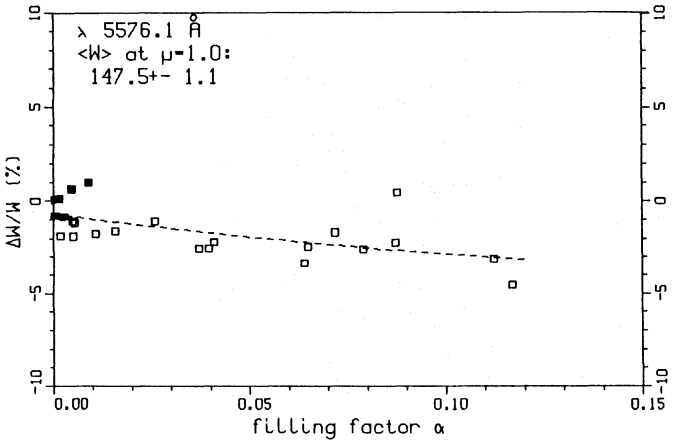

Fig. 6. Change of the equivalent width of the line FeI λ5576.1 Å as a function of the magnetic filling factor α.

lines show almost no change in W with α. Therefore for the strong lines the decrease in area due to the reduced line depth is compensated almost exactly by the increase in line width.

5.5. *Variation of the line asymmetry*

In this section only changes of the shape of the line bisectors will be discussed, while the discussion of possible changes of the line position will be postponed until the next section.

The change of the shape of the line bisectors between quiet Sun and plage regions has been studied by several authors, e.g. Cavallini et al. (1985, 1988), Brandt and Schröter (1984), Immerschitt and Schröter (1987, 1989). However, in the present investigation for the first time two features can be studied in detail: i) whether there is a smooth change of the shape from small to large filling factors, and ii) to what extent this change takes place in different lines.

The typical changes of the bisector shapes for four different lines are shown in Fig. 8a, where full lines represent regions on the solar disk with very small filling factors ($\alpha \ll 0.02$) and squares those with large filling factors ($\alpha > 0.08$). For complementing the discussion of Sect. 5.6, the bisector positions were plotted with reference to the line MgI λ5172.7 Å (cf. Sect. 5.6 for details). One notices the diminished curvature of the "C"–shaped lower parts of the bisectors of the two medium strong lines λ5576.1 Å and λ6252.6 Å, while the 'magnetograph line' λ5250.2 Å indicates a slightly reversed behaviour and the weak line λ5635.8 Å shows no effect at all. Another feature of the bisector change will become apparent in the analysis presented below.

In order to study the behaviour of the upper and the lower parts of the bisectors separately, the following definitions are introduced:

- the wavelength difference between the average of the lowest three bisector points and the point at relative intensity 0.7 (i.e. $\lambda_{min} - \lambda_{0.7}$) is denoted by $\Delta\lambda_\nabla$;
- the wavelength difference between the bisector points at relative intensities 0.7 and 0.9 (i.e. $\lambda_{0.7} - \lambda_{0.9}$) is denoted by $\Delta\lambda_\Delta$.

Thus $\Delta\lambda_\nabla$ is representative for the lower part of the bisector and is by definition positive for a C-shaped bisector, while $\Delta\lambda_\Delta$ represents the upper part of the bisector and usually is negative.

As an example Fig. 9 shows the behaviour of the bisector shape as a function of α for the line λ5576.1 Å. The well known

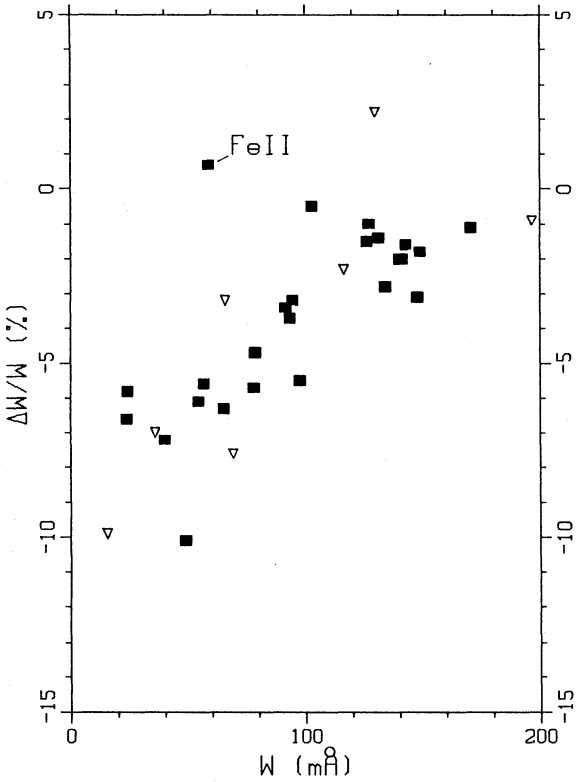

Fig. 7. Change of the equivalent width of all lines of Table 1 between $\alpha < 0.02$ and $\alpha = 0.12$ as a function of the equivalent width. Lines with $\chi_e > 2.0$ eV: squares; lines with $\chi_e \leq 2.0$ eV: triangles.

flattening of the bisector in the *lower part* shows up clearly by the smooth decrease of $\Delta\lambda_\nabla$ from +4 mÅ for $\alpha < 0.02$ to ≈ 0 mÅ for $\alpha = 0.12$. The values of $\Delta\lambda_\nabla$ for $\alpha < 0.02$, called $\Delta\lambda_{\nabla q}$, where 'q' stands for 'quiet', and those for $\alpha = 0.12$, denoted $\Delta\lambda_{\nabla a}$ ('active'), are given for all lines in the last two columns of Table 1. For the *upper part* of the bisector, on the other hand, a small but significant *increase* of $\Delta\lambda_\Delta$ from −7 mÅ to −8 mÅ is indicated for the line λ5576.1 Å.

For a synoptic presentation of the bisector shape behaviour, $\Delta\lambda_\nabla$ (circles) and $\Delta\lambda_\Delta$ (squares) for $\alpha < 0.02$ are plotted in Fig. 10 as a function of the equivalent width of all FeI lines. The change from $\alpha < 0.02$ to maximum α is marked by vertical bars in this graph. The figure confirms the behaviour indicated in the previous one: most of the medium-strong FeI lines have a $\Delta\lambda_\nabla$ between +4 mÅ and +6 mÅ for $\alpha < 0.02$ which decreases to approx. +2 to 0 mÅ for $\alpha = 0.12$, i.e. the bisector straightens considerably in its lower part. This straightening appears to increase with W, being most pronounced for lines with $W \geq 100$ mÅ. A part of this dependence may be due to the definition of $\Delta\lambda_\nabla$, which makes it somewhat dependent on line depth. As a new feature one notices a pronounced *increase* of $\Delta\lambda_\Delta$ for the medium-strong lines with increasing α, the bisector steepens in its upper part by nearly the same amount, corresponding to an increased redshift. This behaviour has not been noticed in previous investigations (e.g. Cavallini et al., 1987; Immerschitt and Schröter, 1987, 1989), although an indication is present in the results by Cavallini et al. (1988). This effect apparently can only be assessed unambiguously by observing many lines with a high S/N ratio, as was done in this analysis. It is largest for lines in the range $80 \lesssim W \lesssim 150$ mÅ. Since the

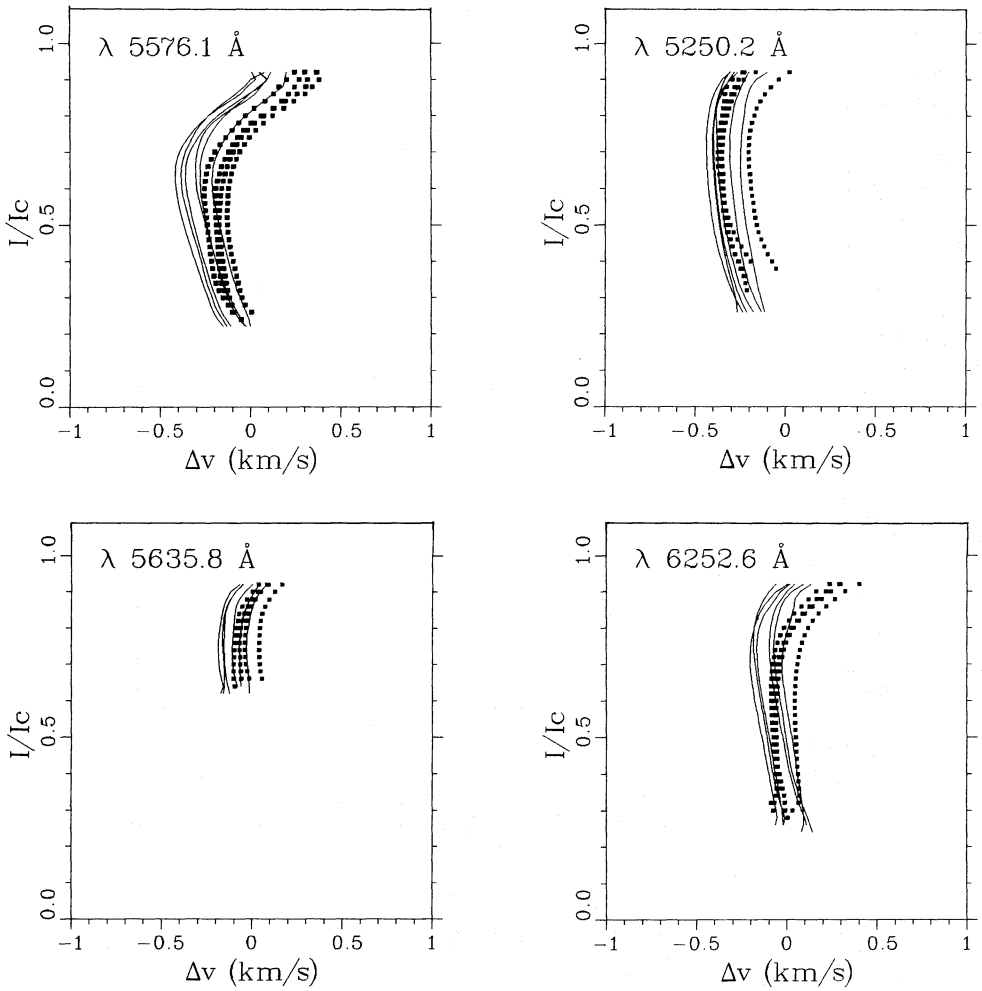

Fig. 8. Typical bisector shapes and positions of FeI lines λ5576.1 Å, λ5250.2 Å, λ5635.8 Å, and λ6252.6 Å of regions with filling factors $\alpha < 0.02$ (full lines) and $\alpha > 0.08$ (squares). The bisector wavelength positions are referred to the MgI line λ5172.7 Å (cf. Sect. 5.6).

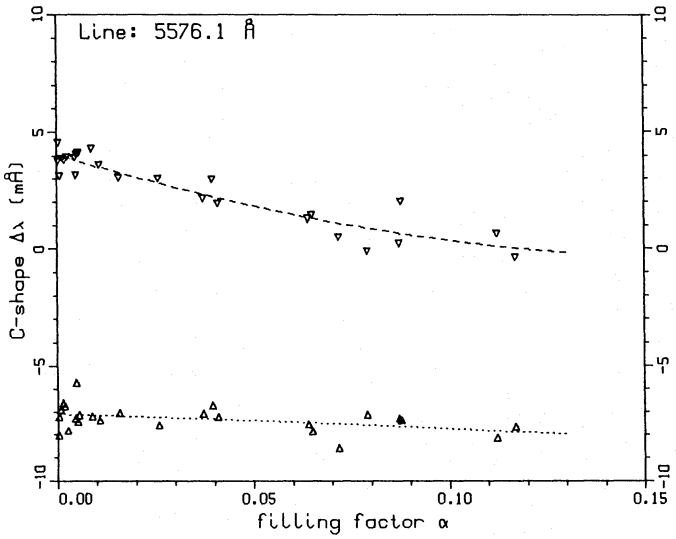

Fig. 9. Bisector shape as a function of the filling factor α for the line FeI λ5576.1 Å. Symbols: $\nabla = \Delta\lambda_\nabla$ = wavelength difference in the lower part of the bisector; $\Delta = \Delta\lambda_\Delta$ = wavelength difference in the upper part of the bisector; for definition cf. text.

bisector values between two fixed levels in the intensity scale are used to parameterise the asymmetry of the upper portion of the line, this definition should be independent of the line strength.

If one plots the bisector shapes and their changes as a function of the Landé factor of the lines, as was done in Fig. 11, one notices that those lines with g values ≥ 2.5 (like the 'magnetograph' line λ5250.2 Å) tend to have reduced curvature in the lower part of the profile and very little change from $\alpha < 0.02$ to high α. This effect was observed before by Brandt and Schröter (1984) and may be caused by contributions of Zeeman split components from the flux tubes shifted in λ due to the missing blueshift. However, since λ5250.2 Å is also a relatively weak line ($W \approx 70$ mÅ), this effect may simply be due to its W. Notice that it fits quite well with the other lines in Fig. 10.

A set of 10 FeI lines of similar strength was used by Livingston (1983, 1987) to investigate possible long term changes of the bisector shape in integrated sunlight. Because these lines are also included in the present analysis, we can study their systematic change with varying filling factor α for regions of $\cos\theta \geq 0.9$ from which an appreciable fraction of the solar radiation comes, and thus can 'calibrate' the bisector change in terms of α. Fig. 12 shows the mean bisector curvatures in the lower part (∇) and upper part (Δ) of the line profiles as

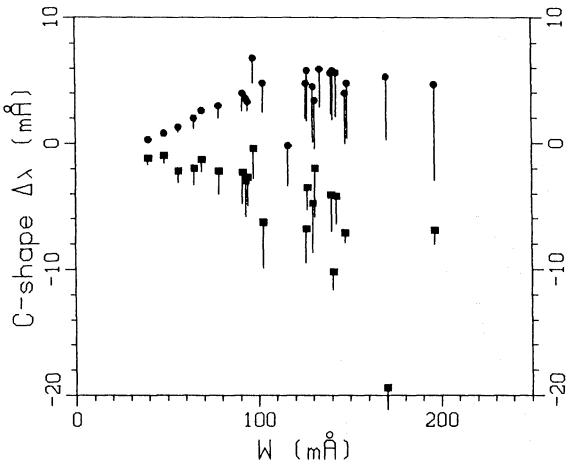

Fig. 10. Change of the bisector shape between $\alpha < 0.02$ and $\alpha = 0.12$ as a function of the equivalent width.

Symbols: • = $\Delta\lambda_V$ for $\alpha < 0.02$; ▪ = $\Delta\lambda_\Delta$ for $\alpha < 0.02$; vertical bars denote change with α increasing to 0.12.

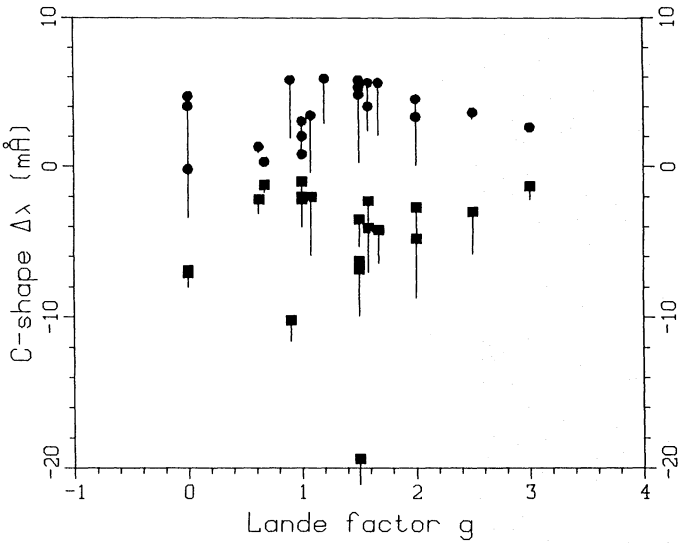

Fig. 11. Change of the bisector shape between $\alpha < 0.02$ and $\alpha = 0.12$ as a function of the Landé factor. Symbols same as in Fig. 10.

a function of α. Our definition of $\Delta\lambda$ and the one used by Livingston (1983, 1987) are almost identical and the results, therefore, well comparable. One notices the conspicuous decrease of the curvature in the lower part of the line from +5 mÅ to $\approx$ +1 mÅ for α varying between 0 and 0.12, as well as the distinct increase in curvature in the upper part mentioned earlier.

5.6. *Variation of the bisector wavelength position*

For a sub-set of 19 FeI lines (cf. Table 1) average bisector wavelength positions were determined in a way similar to the one described by Livingston (1983). In each spectrum the wavelength position of the MgI line λ5172.7 Å was determined by fitting a second order polynomial to the line bottom. From the difference of this wavelength to the value tabulated by Pierce and Breckinridge (1973), the velocity correction due to the combined effect of the earth's orbital motion, terrestrial rotation and solar

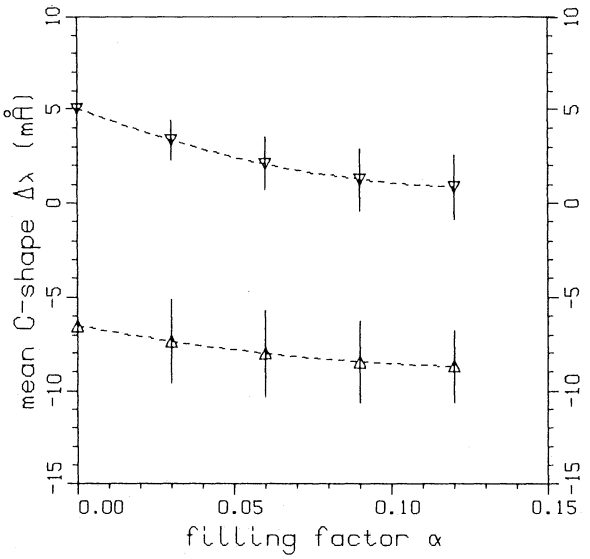

Fig. 12. C-shape averaged over 10 FeI lines as function of α. The set of lines was originally selected by Livingston (1983). Symbols: ∇ = $\Delta\lambda_V$ = average wavelength difference in the lower part of the bisector; Δ = $\Delta\lambda_\Delta$ = average wavelength difference in the upper part of the bisector; for definitions cf. text.

Table 2. Number of spectra observed at $\cos\theta \geq 0.95$ used for averaging FeI line bisectors within different filling factor classes (α in %).

range	$0 \leq \alpha < 1$	$1 \leq \alpha < 4$	$4 \leq \alpha < 8$	$8 \leq \alpha < 12$
number	8	3	3	3

rotation was computed and applied to the 19 solar lines. The strong MgI line was chosen because the granular blue shift is absent in the core of this line (Pierce and Breckinridge, 1973, their Fig. 9). In a two step process the bisectors were then averaged, i) over the sub-set of 19 lines and ii) within groups of spectra with increasing α, as indicated in Table 2. Thus for the $\alpha < 1\%$ group of spectra 8 times 19, or 152 line bisectors were averaged, for the other groups 57. The results are shown in Fig. 13. For the following discussion all line shifts were converted into velocities using the average wavelength for the wavelength interval. For very small filling factors ($\alpha < 1\%$) Fig. 13 shows a blue shift of $\approx$ 0.35 km/s for the intermediate part of the lines ($I/I_c = 0.6$). With α increasing to $\lesssim$ 8% this blue shift decreases to 0.12 km/s at the same intensity level; in the upper half of the bisector an increased redshift is seen. A slight increase of the blue shift is indicated for the three spectra with $\alpha > 8\%$, which may not be significant, however, taking into consideration the width of the $\pm 1\sigma$ error bars. Some examples of the reduced blueshift are shown in Fig. 8. However, note that the wavelength difference at intensity minimum is generally smaller than the values quoted above.

6. Discussion and simple model calculations

6.1. *Line width, line depth, and equivalent width*

Our data clearly show an increase in FWHM with increasing α, even after Zeeman broadening has been compensated for.

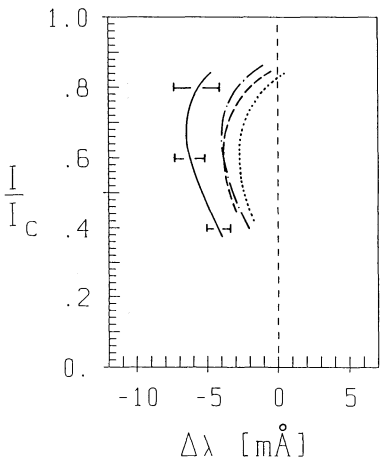

Fig. 13. Line bisectors referred to the wavelength of MgI λ5172.7 Å averaged over 19 FeI lines and groups of spectra with increasing magnetic filling factor α (for details cf. text and Table 1). The $\pm 1\sigma$ error bars are given for the most blue shifted bisector.

Symbols: ——— $\Rightarrow \alpha < 1\%$; $-\cdot-\cdot- \Rightarrow 1\% \leq \alpha < 4\%$; ····· $\Rightarrow 4\% \leq \alpha < 8\%$; – – – – $\Rightarrow \alpha \geq 8\%$.

Therefore, the change in line width, which is largest for the strongest lines, must be due to the different temperature and/or velocity structure in active regions.

Can the increased line width be explained by very broad profiles inside the magnetic elements ? The majority of the lines in our sample show an increase in width of 4–9% due to non-magnetic causes when the filling factor increases by approximately 12%. This would require the profiles in the magnetic elements to be broader than in the quiet Sun by approximately 40%, contradicting observations of Stokes V profiles which show that the line widths within magnetic elements are similar to those in the quiet Sun, if the Zeeman broadening is removed as in Sect. 5.3 (e.g. Solanki and Stenflo, 1984; Solanki, 1986). Consequently, the present observations can only be explained if *the line profiles in the non-magnetic part of an active region grow broader with increasing filling factor.*

Could the observed increase in line width ($\Delta F/F$) be a result of larger velocity fluctuations in the non-magnetic surroundings? Theoretically we expect the magnetic field to inhibit the convection (e.g. Gough and Taylor, 1966; Hurlburt and Weiss, 1987) and theoretical models of magnetic elements assume a decrease in the strength of the convection in their proximity (e.g. Spruit, 1977; Deinzer et al., 1984a,b; Knölker et al., 1988). The observational material in the literature often supports this picture. For example the straightening of the lower half of the bisector in active regions supports the theoretical view. Although Mattig and Nesis (1976) find *increased* r.m.s. fluctuations of the line of sight velocity in plage regions, a more recent analysis of high spatial resolution spectrograms by Nesis et al. (1989) contradicts this result, as do observations by Title et al. (1986, 1989), who find increased lifetimes as well as decreased *horizontal* velocities in active regions — facts which hint at reduced dynamics, including reduced *vertical* velocities, in active regions.

However, it is possible to qualitatively explain the observations with the following scenario: The line broadening velocities are concentrated into smaller scales, below even the excellent resolution of the observations of Nesis et al. (1989). If this is coupled to a decrease in the temperature contrast between rising and falling blobs of matter then it may also be able to explain the straightening of the lower part of the line bisector. Possible support for higher downflow velocities in active regions is provided by the increased redshift of the upper part of the line bisector (although this may simply be due to increased weighting of light from the downflow component as the continuum contrast between upflow and downflow is reduced).

Another possible explanation is that the line profiles from the non-magnetic component of an active region are broader due to increased saturation, produced by a lower temperature. A cooling of the non-magnetic part of an active region atmosphere is theoretically expected as a result of the inhibition of convection and the influx of heat into the magnetic elements (e.g. Spruit, 1977; Deinzer et al., 1984a,b).

The line width is not the only observed parameter. Line profiles resulting from the correct hypothesis must also reproduce the observed line depths, equivalent widths and bisectors. Let us now consider the line depths and equivalent widths.

The weakening of spectral lines in active regions and in the supergranular network is well known. Thermal weakening in the hot magnetic component and, for the more Zeeman sensitive lines, Zeeman splitting are well established as the main causes (e.g. Chapman and Sheeley, 1968; Harvey and Livingston, 1969; Harvey et al., 1972; Frazier and Stenflo, 1978; Schüssler and Solanki, 1988) and are also supported by our observations. The decrease in equivalent width with filling factor can be considered to be primarily a result of the decrease in line depth, but is smaller since the effect of the latter is partially offset by the increase in line width, particularly for strong lines.

It is always possible to find some combination of broadening velocities and fluxtube temperature which reproduces the observed line profiles. However, the temperature within the magnetic elements is not completely unknown. We have a fairly good idea of what the line profiles formed within flux tubes look like. This greatly restricts the freedom of choice of velocity fluctuations. However, we do not consider the case for increased line broadening velocity further and turn now to the other, more interesting, proposal.

We have tested whether the observed trends of the line parameters can be qualitatively reproduced by a lower temperature in the non-magnetic component of an active region as compared to the quiet Sun. A number of hypothetical FeI lines with different equivalent widths were calculated, using a Stokes radiative transfer code (Solanki, 1987b) based on the technique described by Beckers (1969), for a simple two-component model of an active region. The magnetic component is simply taken to be represented by the network model of Solanki (1986) with the line broadening velocity chosen such that the widths of the observed Stokes V profiles are reproduced. For the non-magnetic atmosphere we initially chose a series of models with $T(\tau)$ parallel to that of the HSRA. All the models were cooler than the HSRA. The line profiles were calculated along a single ray in each component and then weighted according to the filling factors of the two components before being summed to give the average active region Stokes I profile. No combination of filling factor and temperature was found, which could reproduce the observations.

However, if a non-magnetic atmosphere with a flatter temperature stratification is chosen, then it is possible to obtain good qualitative agreement with the data, namely the decrease in line

depth and equivalent width (mainly for weaker lines) and the increase in line width (mainly for stronger lines).

Whether the smaller temperature gradient in the non-magnetic atmosphere is a real effect is arguable, since magnetic elements expand with height and are hotter than the quiet Sun. Any model not taking this expansion into account will show a too small $T(\tau)$ gradient. Only extensive 2-D models will be able to decide how strong this effect is.

It appears, according to this model, that in the lower part of the photosphere, where the line wings and flanks are formed, the average temperature in the non-magnetic part of an active region is lower by approximately 50 to 100 K than in the quiet Sun. This is in excellent agreement with the continuum intensity of 0.9 times the quiet Sun intensity found by Schüssler and Solanki (1988) for the non-magnetic component of an active region. In the upper photosphere, the model predicts that the non-magnetic atmospheric component becomes warmer than the quiet Sun, but this result appears considerably less trustworthy (see previous paragraph).

Note, that if we were to neglect the difference in thermal structure between the quiet Sun and the non-magnetic component of a plage and were then to derive the temperature of the magnetic component from low spatial resolution Stokes I profile observations, then the above results suggest that we would obtain a sharp rise in the temperature difference between magnetic component and the quiet Sun with height. This appears to be a promising way of reconciling models of magnetic elements derived from low resolution Stokes I profiles (e.g. Chapman, 1979; Walton, 1987) and from Stokes V profiles (e.g. Solanki, 1986; Keller, 1989; Keller et al., 1989). See also the more extended discussion on this topic by Solanki (1989).

The second explanation, i.e. a decrease in temperature of the lower part of the non-magnetic atmosphere in active regions, fits both current theoretical ideas (cool ring around flux tubes; cf. Spruit, 1977; Deinzer et al., 1984a,b; Knölker and Schüssler, 1988) and other observations (e.g. Schüssler and Solanki, 1988) better than the first explanation. Therefore, although we cannot discount the first explanation, we feel that the second is to be preferred.

6.2. *Line bisectors*

In agreement with the data published in the literature (e.g. Livingston, 1982, 1983; Kaisig and Schröter, 1983; Miller et al., 1984; Cavallini et al., 1985, 1988; Immerschitt and Schröter, 1989; Keil et al., 1989) we observe a straightening of the lower part of the bisector of lines with a sizeable line depth ($d > 0.7$ in the quiet Sun) as the filling factor increases. However, we, for the first time, also present reliable evidence for the fact that for many lines the upper part of the line bisector steepens (i.e. becomes more horizontal) so that the part of the line near the continuum is redshifted compared to the quiet Sun.

Three empirical models have so far been proposed to explain changes in line bisectors caused by the magnetic field (Miller et al., 1984; Cavallini et al., 1987; Immerschitt and Schröter, 1989). In the following we briefly discuss the promising model of Immerschitt and Schröter (1989) and how it may apply to our observations. They assume three components for an active region: fluxtubes with no stationary flow, a bright upflowing non-magnetic component, and a dark downflowing non-magnetic component. As they increase the area factor of the fluxtube component, they decrease the area factor of the upflowing component proportionally. With this simple model they can explain their observations of changes in the line bisector and other line parameters of FeI λ5576.1 $\AA$ with increasing CaII-K flux. Since they do not change the velocities in the non-magnetic components, a direct interpretation of their model is unphysical. It does not conserve mass in active regions. However, if we interpret the changes in their 'area factors' of the non-magnetic parts mainly as changes in continuum brightness (which cannot be easily distinguished from area factors in low spatial resolution observations, e.g. Schüssler and Solanki, 1988), then their model appears a promising way of explaining changes in line bisectors with increasing α. A decreased continuum contrast between the up- and downflowing non-magnetic parts of an active region is exactly what is expected from "abnormal granulation" as observed in the vicinity of filigree by e.g. Dunn and Zirker (1973) and near magnetic fields by e.g. Ramsey et al. (1977). A decrease in continuum contrast, i.e. in the temperature fluctuations, also implies a decrease in the absolute brightness of the non-magnetic component, in agreement with the results of the model calculations described in Sect. 6.1. Note, that due to the high continuum intensity of the magnetic elements (Schüssler and Solanki, 1988), the total intensity of the active region need not decrease with increasing magnetic filling factor. Our data and simple model calculations together with the model calculations of Immerschitt and Schröter (1989) suggest that the decrease in contrast of the abnormal granulation is not just due to a filling up of the intergranular lanes with magnetic elements, but also due to the decrease in the absolute brightness of the granule centres.

The large redshift of the upper parts of the bisectors may be due to the presence of sizeable downflows in the non-magnetic part of the active regions, over and above the usual granular downflow, perhaps as a result of "baroclinic" cells, adjacent to flux tubes, produced by the inflow of radiation into the magnetic elements (Deinzer et al., 1984a,b; Knölker et al., 1988). However, the redshifts of the upper part of the bisectors could also be an effect of the increased weighting of the granular downflow component due to the decrease in the contrast between the upflow and downflow components.

Can the observations of cycle dependent bisector variations of the Sun observed 'as a star' be explained by the effect of plages? An estimate of the order of magnitude of bisector change shows that the global magnetic filling factor must change by at least 0.005, a substantial fraction of the global filling factor, in order to cause the bisector curvature to decrease by approx. 0.3 mÅ, the value found by Livingston (1983, 1987).

An interesting possibility is to search for bisector changes due to magnetic activity on late type stars. Since some stars may easily have the filling factors and field strengths found in solar active regions, when averaged over their whole visible surface (e.g. Robinson et al., 1980; Marcy, 1984; Gray, 1984; Saar and Linsky, 1985; Saar, 1987; Mathys and Solanki, 1989), it should be possible to observe such changes, despite the lower S/N ratios and generally lower spectral resolution ($\lambda/\Delta\lambda < 100000$) of stellar observations. Our results suggest that strong lines are most likely to show an observable effect, with FeI λ5576.1Å being a good candidate, although not the only promising line.

6.3. *Wavelength shift*

The determination of absolute bisector wavelength positions and shifts is a very difficult observational task, because it

requires an extremely reliable absolute wavelength scale, accurate positioning on the Sun, and moreover, if the measurements are performed away from disk centre, the elimination of the unknown horizontal velocity component of the supergranulation. The method described in Sect. 5.6 (first introduced by Livingston, 1983) avoids most of these difficulties, makes use of the accurate wavelength scale of the FTS, and, due to averaging over many lines, reduces the errors to $\lesssim \pm 0.06$ km/s. The amount of blue shift of 0.35 km/s found here for medium-strong lines in regions of small filling factors is in excellent agreement with the results by Pierce and Breckinridge (1973) and Dravins et al. (1981), but disagrees with the recent findings by Keil et al. (1989), who find no shift of the line core at all. Here we show the systematic reduction of this blue shift to ≤ 0.1km/s with the filling factor α increasing to ≥ 0.08. Howard (1971, 1972) interpreted this reduced blue shift in his Doppler compensator velocity measurements as large scale downward flows in active regions — leaving open the question of where this mass comes from. Similarly, the very large scale velocity features of 20 to 40 m/s amplitude described by Howard (1979) may be attributed to the influence of slight magnetic activity (α of a few %) creating a line shift. Instead of explaining the latter experimental findings by large scale vertical or horizontal transport of material, one should search for the origin of this effect in a modification of the intensity-velocity correlation of the convective pattern in active regions. Both the reduced intensity contrast of the "abnormal granulation" (Edmonds, 1960; Dunn and Zirker, 1973) and the reduced dynamics (Title et al., 1986, 1989; Nesis et al., 1989) in these regions of non-zero filling factors contribute to a reduction of the blue shift as measured here.

7. Conclusion

We have presented the results of an analysis of high quality FTS spectra, obtained in facular regions near solar disk centre, having different amounts of magnetic flux or, equivalently, different filling factors, α. The line parameters (depth, width, equivalent width, wavelength, bisector shape) of 32 spectral lines and their variation with α have been studied. Besides the well established decrease of line depth and equivalent width with increasing α (e.g. Sheeley, 1967; Stenflo and Harvey, 1985), we have also found evidence for an increased line width. In contrast to the line depth, which is reduced mainly for weak lines, it is the stronger lines which exhibit the largest increase in line width. Since the line profiles formed *within* the magnetic elements are not significantly broader than in the quiet Sun (e.g. Solanki, 1986), the profiles formed in the non-magnetic *surroundings* of magnetic elements must instead be broadened. The line bisectors have been observed to evolve steadily with increasing α. In accordance with previous studies (e.g. Cavallini et al., 1985; Immerschitt and Schröter, 1989) we have found the lower part of the bisector to straighten with increasing α. However, unlike previous authors we have also observed that the upper part of the line bisector of many lines becomes more horizontal and redshifted. Finally, the blueshift of the line cores decreases slightly with increasing α. In this respect our observations agree with those of Cavallini et al. (1985) and Immerschitt and Schröter (1989), but contradict those of Kaisig and Schröter (1983) and Keil et al. (1989).

We have attempted to qualitatively understand the consequences of our observations with the help of simple model calculations and by comparison with models published in the literature, mainly those of Immerschitt and Schröter (1989). Consider a model with three components of which one component, representing the hot magnetic flux tubes, is fixed by observations of Stokes V profiles (cf. Solanki, 1989, for a review of properties of flux tubes). Then our observations can be qualitatively explained by the following changes (with respect to the quiet Sun) in the components representing the up- and downflowing non-magnetic components. The bisector changes imply mainly a reduction in the continuum contrast between the upflowing and the downflowing non-magnetic material, although an increase in the downflow velocities in the vicinity of flux tubes, as suggested by the calculations of Deinzer et al. (1984a,b), cannot be ruled out. In white light images or in filtergrams the granulation giving rise to the distorted bisectors will appear "abnormal" (Dunn and Zirker, 1974; Ramsey et al., 1977). In addition, the observed combination of decreased line depths and equivalent widths (mainly for weaker lines) and increased line widths (mainly for stronger lines), in our opinion, requires the temperature in the lower photosphere, averaged over both the non-magnetic components, to be 50–100 K lower than in the quiet Sun for a filling factor of 10–20%. This is in good agreement with the empirical results of Schüssler and Solanki (1988) and with theoretical model calculations (Spruit, 1977; Deinzer et al., 1984a,b; Knölker et al., 1987; Grossmann-Doerth et al., 1989). Such a temperature reduction is also a natural outcome of the reduced granular continuum contrast, due to energy conservation. We can therefore rule out the idea that the abnormal granulation is mainly the result of the dark intergranular lanes of normal granulation being filled by bright magnetic elements. We find that the properties of the convective cells themselves change considerably in the vicinity of magnetic features.

Acknowledgements. We thank J. Brault, B. Graves, R. Hubbard and G. Ladd of the N.O.A.O. (Tucson) for assistance in the operation of the McMath telescope and the FTS system, and for carrying out the data transformation. The National Optical Astronomy Observatories are operated by the Association of Universities for Research in Astronomy, Inc., under contract to the National Science Foundation. Moreover, we are indebted to M. Steinegger (Graz) for help in the data evaluation and to H. P. Schilling for his assistance in preparing the manuscript. We also wish to thank E.-H. Schröter for critically reading the manuscript and helping to improve the presentation. One of us (P.N.B.) gratefully acknowledges financial support from the Deutsche Forschungsgemeinschaft.

References

Babcock, H.D., Herzberg, L.: 1948, *Astrophys. J.* **108**, 167
Balthasar, H.: 1984, *Ph. D. Thesis*, Göttingen University
Beckers, J.M.: 1969, *Solar Phys.* **9**, 372
Beckers, J.M., Nelson, G.D.: 1978, *Solar Phys.* **58**, 243
Beckers, J.M., Schröter, E.H.: 1968, *Solar Phys.* **4**, 142
Brandt, P.N., Nesis, A.: 1973, *Solar Phys.* **31**, 75
Brandt, P.N., Schröter, E.-H.: 1984, *Small-Scale Dynamical Processes in Quiet Stellar Atmospheres*, ed. S. Keil, NSO Conf., 371
Brandt, P.N., Solanki, S.K.: 1987, *The Role of Fine-Scale Magnetic Fields on the Structure of the Solar Atmosphere*, eds. E.-H. Schröter, M. Vazquez, A.A. Wyller, Cambridge Univ. Press, 82

Brault, J.W.: 1978, *Proc. JOSO Workshop: Future Solar Optical Observations — Needs and Constraints*, eds. G. Godoli, G. Noci, A. Righini, Osserv. Mem. Oss. Astrofis. Arcetri, No. 106, 33
Brault, J.W.: 1985, *High Resolution in Astronomy*, 15th Advanced Course of the Swiss Society of Astrophysics and Astronomy, Saas-Fee 1985, eds. A. Benz, M. Huber, M. Mayor, Geneva, 1
Brault, J.W., White, O.R.: 1971, *Astron. Astrophys.* **13**, 169
Cavallini, F., Ceppatelli, G., Righini, A.: 1985, *Astron. Astrophys.* **143**, 116
Cavallini, F., Ceppatelli, G., Righini, A.: 1987, *Astron. Astrophys.* **173**, 155
Cavallini, F., Ceppatelli, G., Righini, A.: 1988, *Astron. Astrophys.* **205**, 278
Chapman, G.A.: 1970, *Solar Phys.* **14**, 315
Chapman, G.A.: 1979, *Astrophys. J.* **232**, 923
Chapman, G.A., Sheeley, N.R. Jr.: 1968, *Solar Phys.* **5**, 442
Deinzer, W., Hensler, G., Schüssler, M., Weisshaar, E.: 1984a, *Astron. Astrophys.* **139**, 426
Deinzer, W., Hensler, G., Schüssler, M., Weisshaar, E.: 1984b, *Astron. Astrophys.* **139**, 435
Delbouille, L., Neven, L., Roland, G.: 1973, *Photometric Atlas of the Solar Spectrum from λ 3000 to λ 10000*, Liege.
Dravins, D., Lindegren, L., Nordlund, A.: 1981, *Astron. Astrophys.* **96**, 345
Dravins, D., Larsson, B., Nordlund, A.: 1986, *Astron. Astrophys.* **158**, 83
Dravins, D.: 1987, *Astron. Astrophys.* **172**, 211
Dunn, R.B., Zirker, J.B.: 1973, *Solar Phys.* **33**, 281
Edmonds, F.N.: 1960, *Astrophys. J.* **131**, 57
Frazier, E.N., Stenflo, J.D.: 1978, *Astron. Astrophys.* **70**, 789
Gough, D.O., Taylor, R.J.: 1966, *Monthly Notices Roy. Astron. Soc.* **133**, 85
Gray, D.F.: 1982, *Astrophys. J.* **255**, 200
Gray, D.F.: 1984, *Astrophys. J.* **277**, 640
Griffin, R.F.: 1969, *Monthly Notices Roy. Astron. Soc.* **143**, 361
Grossmannn-Doerth, U., Pahlke, K.-D., Schüssler, M.: 1987, *Astron. Astrophys.* **176**, 139
Grossmann-Doerth, U., Knölker, M., Schüssler, M., Weisshaar, E.: 1989, *Solar and Stellar Granulation*, Proc. Nato Adv. Res. Workshop, Capri, June 21-25, eds. R. J. Rutten and G. Severino, Kluwer, Dordrecht
Harvey, J.W., Livingston, W.C.: 1969, *Solar Phys.* **10**, 283
Harvey, J.W., Livingston, W.C., Slaughter, C.: 1972, *Line Formation in the Presence of Magnetic Fields*, High Altitude Obs., NCAR, Boulder, CO, 227
Howard, R.: 1971, *Solar Phys.* **16**, 21
Howard, R.: 1972, *Solar Phys.* **24**, 123
Howard, R.: 1979, *Astrophys. J.* **228**, L45
Hughes, D.W., Proctor, M.R.E.: 1988, *Ann. Rev. Fluid Mech.* **20**, 187
Hurlburt, N.E., Weiss, N.O.: 1987, *The Role of Fine-Scale Magnetic Fields on the Structure of the Solar Atmosphere*, eds. E.-H. Schröter, M. Vazquez, A.A. Wyller, Cambridge Univ. Press, 35
Immerschitt, S., Schröter, E.-H.: 1987, *The Role of Fine-Scale Magnetic Fields on the Structure of the Solar Atmosphere*, eds. E.-H. Schröter, M. Vazquez, A.A. Wyller, Cambridge Univ. Press, 53
Immerschitt, S., Schröter, E.-H.: 1989, *Astron. Astrophys.* **208**, 307
Kaisig, M., Durrant, C.J.: 1982, *Astron. Astrophys.* **116**, 332
Kaisig, M., Schröter, E.-H.: 1983, *Astron. Astrophys.* **117**, 305
Keil, S.L., Roudier, Th., Cambell, E., Koo, B.C., Marmolino, C.: 1989, *Solar and Stellar Granulation*, Proc. Nato Adv. Res. Workshop, Capri, June 21-25, eds. R. J. Rutten and G. Severino, Kluwer, Dordrecht, 273
Keller, C.U.: 1989, *Solar Photosphere: Structure, Convection and Magnetic Fields*, IAU Symp. No. 138, Kiev, May 15–20, 1989, in press
Keller, C.U., Solanki, S.K., Steiner, O., Stenflo, J.O.: 1989, *Astron. Astrophys.* submitted
Knölker, M., Schüssler, M.: 1988, *Astron. Astrophys.* **202**, 275
Knölker, M., Schüssler, M., Weisshaar, E.: 1988, *Astron. Astrophys.* **194**, 257
Koutchmy, S.: 1977, *Astron. Astrophys.* **61**, 397
Kurucz, R.L., Furenlid, I., Brault, J., Testerman, L.: 1984, *Solar Flux Atlas from 296 to 1300 nm*, National Solar Obs., Sunspot, NM
Landi Degl'Innocenti, E.: 1982, *Solar Phys.* **77**, 285
Landi Degl'Innocenti, E.: 1985, *Solar Phys.* **99**, 1
Livingston, W.C.: 1982, *Nature* **297**, 208
Livingston, W.C.: 1983, *Solar and Stellar Magnetic Fields: Origins and Coronal Effects*, ed. J.O. Stenflo, IAU, Symp. 102, 149
Livingston, W.C.: 1984, *Small-Scale Dynamical Processes in Quiet Stellar Atmospheres*, ed. S. Keil, NSO Conf., 330
Livingston, W.C.: 1987, *The Role of Fine-Scale Magnetic Fields on the Structure of the Solar Atmosphere*, eds. E.-H. Schröter, M. Vazquez, A.A. Wyller, Cambridge Univ. Press, 14
Livingston, W.C., Holweger, H.: 1982, *Astrophys. J.* **252**, 375
Livingston, W.C., Huang, Y.-R.: 1986, *The SHIRSOG Workshop*, NOAO, Tucson, Arizona, Sept. 3, 1986, ed. M.S. Giampapa, 1
Marcy, G.W.: 1984, *Astrophys. J.* **281**, 286
Mathys, G., Solanki, S.K.: 1989, *Astron. Astrophys.* **208**, 189
Mathys, G., Stenflo, J.O.: 1986, *Astron. Astrophys.* **168**, 184
Mattig, W., Nesis, A.: 1976, *Solar Phys.* **50**, 255
Miller, P., Foukal, P., Keil, S.: 1984, *Solar Phys.* **92**, 33
Moore, C.E., Minnaert, M.G.J., Houtgast, J.: 1966, *Second Revision of Rowlands Preliminary Tables*, NBS Monograph 61
Muller, R., Keil, S.L.: 1983, *Solar Phys.* **87**, 243
Nesis, A., Fleig, K.-H., Mattig, W.: 1989, *Solar and Stellar Granulation*, Proc. Nato Adv. Res. Workshop, Capri, June 21-25, eds. R. J. Rutten and G. Severino, Kluwer, Dordrecht
Nordlund, A.: 1986, *Small Magnetic Flux Concentrations in the Solar Photosphere*, eds. W. Deinzer, M. Knölker, H.H. Voigt, Vandenbeck & Ruprecht, Göttingen, 83
Palmer, B.A., Engleman, R. Jr.: 1983, *Atlas of the Thorium Spectrum*, Los Alamos Natl. Lab.
Pierce, A.K, Breckinridge, J.B.: 1973, Kitt Peak National Obs. Contr. No. 559
Ramsey, H.E., Schoolman, S.A., Title, A.M.: 1977, *Astrophys. J.* **215**, L41
Robinson, R.D., Worden, S.P., Harvey, J.W.: 1980, *Astrophys. J.* **236**, L155
Saar, S.H.: 1987, Ph. D. Thesis, University of Colorado, Boulder
Saar, S.H., Linsky, J.L.: 1985, *Astrophys. J.* **299**, L47
Schröter, E.-H.: 1957, *Z. Astrophys.* **41**, 141
Schüssler, M., Solanki, S.K.: 1988, *Astron. Astrophys.* **192**, 338
Sheeley, N.R.: 1967, *Solar Phys.* **1**, 171
Solanki, S.K.: 1985, *Theoretical Problems in High Resolution Solar Physics*, ed. H.U. Schmidt, Max-Planck-Inst. f. Astrophys., Munich, 172

Solanki, S.K.: 1986, *Astron. Astrophys.* **168**, 311
Solanki, S.K.: 1987a, *The Role of Fine-Scale Magnetic Fields on the Structure of the Solar Atmosphere*, eds. E.-H. Schröter, M. Vazquez, A.A. Wyller, Cambridge Univ. Press, 67
Solanki, S.K.: 1987b, Ph. D. Thesis, ETH Zürich, No. 8309
Solanki, S.K.: 1989, *Solar Photosphere: Structure, Convection and Magnetic Fields*, IAU Symp. No. 138, Kiev, May 15–20, 1989, in press
Solanki, S.K., Stenflo, J.O.: 1984, *Astron. Astrophys.* **140**, 185
Solanki, S.K., Stenflo, J.O.: 1985, *Astron. Astrophys.* **148**, 123
Solanki, S.K., Zayer, I., Stenflo, J.O.: 1989, *High Resolution Solar Observations*, ed. O. v.d. Lühe, in press
Spruit, H.: 1977, *Solar Phys.* **55**, 3
Stenflo, J.O., Harvey, J.W.: 1985, *Solar Phys.* **95**, 99
Stenflo, J.O., Harvey, J.W., Brault, J.W., Solanki, S.K.: 1984, *Astron. Astrophys.* **131**, 333
Stenflo, J.O., Lindegren, L.: 1977, *Astron. Astrophys.* **59**, 367
Tarbell, T.D., Title, A.M.: 1977, *Solar Phys.* **52**, 13
Title, A.M., Tarbell, T.D., Simon, G.W., and the SOUP team: 1986, *Adv. Space Res.* Vol. 6, No. 8, 253
Title, A.M., Tarbell, T.D., Topka, K.P., Ferguson, S.H., Shine, R.A. and the SOUP Team: 1989, *Astrophys. J.* **336**, 475
Walton, S.R.: 1987, *Astrophys. J.* **312**, 909
Zayer, I., Solanki, S.K., Stenflo, J.O.: 1989, *Astron. Astrophys.* **211**, 463

This article was processed by the author using Springer-Verlag TEX AA macro package 1989.